Annals of Anatomy 221 (2019) 38–47

Contents lists available at ScienceDirect

Annals of Anatomy

journal homepage: www.elsevier.com/locate/aanat

RESEARCH ARTICLE

# Distribution of the neuropeptide calcitonin gene-related peptide-α of tooth germ during formation of the mouse mandible

Yuuki Maeda [a,b], Yoko Miwa [b], Iwao Sato [b,*]

[a] Division of Anatomy, Nippon Dental University Graduate School of Life Dentistry, Tokyo, Japan
[b] Department of Anatomy, School of Life Dentistry at Tokyo, The Nippon Dental University, Tokyo, Japan

ARTICLE INFO

*Article history:*
Received 8 June 2018
Received in revised form 19 July 2018
Accepted 1 September 2018

*Keywords:*
CGRP
CRLR
Mandible
Tooth germ
Development

ABSTRACT

Calcitonin gene-related peptide-α (CGRPα) is a neurotransmitter that is related to bone formation during development. However, CGRP expression is not well known to affect the formation of teeth during development. During tooth germ development, the relationships among CGRPα, calcitonin receptor-like receptor (CRLR), amelogenin (AMELX), dentin sialophosphoprotein (DSPP), osteopontin (OPN) and osteocalcin (OCN) are unclear despite various tooth and osteogenesis markers. Our real-time RT-PCR results showed that the expression levels of CGRPα mRNA gradually decreased, in contrast to the mRNA abundances of CRLR, AMELX, DSPP, OPN, and OCN, which rapidly increased from E14.5 to P1 in the mandible. *In situ* hybridization using an antisense probe for CGRPα mRNA showed significant localized expression levels around the tooth bud at E14.5 and epithelial cells near the dental ledge and outer and inner enamel epithelium at E17.5 compared to those at P1. The localization of the anti-CGRPα antibody reaction revealed a strong positive reaction at the surface layer of oral epithelial cells at E14.5 and oral epithelial cells of the dental lamina around the dental ledge depression in the mandible of E17.5 mice using immunohistochemical methods The different anti-CGRPα reaction revealed its important roles during tooth formation at the postnatal stage. CGRPα mRNA was also detected in the interactions of tooth germ with the formation of odontoblast and amelobast layers from dental papilla and inner enamel epithelium. CGRPα may also be related to tooth germ development. Furthermore, CGRPα is an important tooth and bone formation marker, and bone cells provide further evidence of a role in mandibular development in contrast to inflammatory systems.



## 1. Introduction

There are two isomers of calcitonin gene-related peptide, calcitonin gene-related peptide-α (CGRPα) and calcitonin gene-related peptide-β (CGRPβ). CGRPα is predominantly distributed in the Aδ and C fibers of the peripheral sensory ganglion, and CGRPβ is mainly distributed in the nervous system of the intestinal tract (Edvinsson and Ho, 2010). Neuropeptide CGRPα is a member of the neuromodulator group that inhibits periosteal development (Hill and Elde, 1991). CGRPα affects acetylcholine receptors at neuromuscular junctions during development (New and Mudge, 1986; Fontaine et al., 1986; Mulle et al., 1988; Miles et al., 1989) and osteoblasts (Cornish et al., 1999; Sisask et al., 2013). In bone metabolism, CGRPα is associated with the bone-forming cells (Hukkanen et al., 1993; Konttinen et al., 1996; Valentijn et al., 1997; Bo et al., 2012; Fang et al., 2013; Maeda et al., 2017) and promotes osteogenesis *in vitro* (Dong et al., 2010; Yoo et al., 2014; Takahashi et al., 2016; Fristad et al., 1994; Nagata et al., 1992); despite this, CGRPα is one of several important mediators of facial inflammation (Multon et al.,2005) and TMJ pain (Haeuchi et al., 1999; Sato et al., 2012). CGRPα is a neurotransmitter that is implicated in various conditions; it is a mediator of facial inflammation (Multon et al., 2005) and migraines (Benemei et al., 2009) and causes neurogenic inflammation (Russell et al., 2011). CGRPα affects the vessels on the surface of the maxillary sinus mucosa (Sato et al., 2012) and affects pain and hearing in the human tensor tympani muscle (Yamazaki and Sato, 2014). Previous immunohistochemical studies have indicated that nerve fibers with CGRPα-immunoreactivity were found in the dental follicle in the bell stage at postnatal day 9. Nerve fibers with CGRPα-immunoreactivity were also found in the basal layer, dental lamina and ameloblasts after the postnatal stage in mice (Nagata et al., 1992, 1994). However, expression of CGRPα was not described in the mandible in previous reports. CGRP expression in tooth formation may relate to the interactions between the ectodermal cells of the jaw epithelium and the underlying neural crest-derived mesenchymal cells during development. We focused on CGRP expression during the bone formation stage with tooth germ in the mandible. CGRPα has no clearly defined association

* Corresponding author at: 1-9-20, Fujimi, Chiyoda-ku, Tokyo 102-0071, Japan.
*E-mail address:* iwaoa1@tky.ndu.ac.jp (I. Sato).

https://doi.org/10.1016/j.aanat.2018.09.001
0940-9602/

between bone formation and tooth germ during development from the embryonic to postnatal stages. In the embryonic stage, CGRP first appears in the mouse at E16.5, localizing around the blood vessels, and is closely associated with the cartilaginous bone matrix in mouse limbs (Bidegain et al., 1995). The osteoclasts and osteogenesis needed for eruption are regulated both chronologically and spatially by differential gene expression levels in the dental follicle (Wise, 2009). The gene expression levels of bone formation markers are associated with tooth eruption in the eruption pathway. Alendronate affects osteoclasts and the expression of the regulatory proteins of the receptor activator of nuclear factor kappa-B ligand in the bone of the first molar germ (Bradaschia-Correa et al., 2013). The neurotransmitters and neuropeptides in bone, including adrenaline, noradrenaline, substance P, CGRPα, vasoactive intestinal peptide and neuropeptide, lead to a direct signaling system between the brain and bone (Bjurholm, 1991; Tabarowski et al., 1996). However, CGRPα has no clearly defined association between bone formation and tooth germ at the embryonic stage in mandibular development in comparison to that of CGRPα with neurotransmitters of nociceptive sensory C fibers. Therefore, we examined the expression levels of CGRPα, CRLR, AMELX, DSPP, OPN and OCN mRNAs of the mandibular body with tooth germ during development to understand the relationships among these organogenesis markers.

## 2. Materials and methods

### 2.1. Sample preparation

All laboratory animals were procured from the Nippon Medical Science Animal Resource Laboratory and were bred at the Animal Testing Centre of the Department of Dentistry, Nippon Dental University. Male mice (CLER JAPAN, Inc.; Tokyo, Japan) were maintained on a solid pellet diet (MF; Oriental Yeast Inc., Tokyo, Japan). Mice at E14.5, E17.5, E18.5, P0 and P1 stages were used (n = 20). The animals were sacrificed using an overdose of pentobarbital, and the right mandible was subsequently removed. Fresh samples were isolated and prepared from the right mandible of the mandibular body with the first molar of the tooth germ and divided into four groups for real-time RT-PCR analysis. Light microscopy studies were conducted on tissues from each stage of the left mandible.

### 2.2. Analysis of mRNA using real-time RT-PCR

#### 2.2.1. Isolation of total RNA

The mandible, containing the mandibular body and molar tooth germ, was removed from each mouse (E14.5, E17.5, E18.5, P0 and P1) by scraping immediately after sacrifice and stored at −80 °C. Each sample was cut into small pieces, and 20–50 mg of total RNA was isolated from the samples using an RNeasy Mini Kit (74104, Qiagen, CA, USA) according to the manufacturer's instructions. Contaminating DNA was removed using RNase-free DNase (DNA-free; Ambion, TX, USA), and the total RNA was quantified using a spectrophotometer (Biowave S2100; Cambridge, UK) at an absorbance wavelength of 260 nm. The samples were stored at −80 °C until further use. Total RNA was converted to cDNA using 0.4 μM random hexamers (N808-0127; Applied Biosystems, CA, USA) in a mixture containing dNTPs at 1 mM each, 20 units of RNase inhibitor (2311A; TaKaRa, Tokyo, Japan), 5 units of AMV reverse transcriptase XL (2620A; TaKaRa), 25 mM Tris–HCl (pH 8.3), 50 mM KCl, 2 mM DTT, and 5 mM $MgCl_2$. The thermal PCR incubation conditions used were as follows: 30 °C for 10 min, 42 °C for 30 min, 90 °C for 5 min, and 5 °C for 5 min. The mandible bone-like connective tissue and molar tooth germ were separated using a microscope (LEICA MZ16, Leica Microsystems, Bensheim, Germany).

**Table 1**
List of reagents.

RT-PCR sequences list

| Abbreviation | Gene number (Gene name) | Source |
|---|---|---|
| CGRPα | Mm00801463_g1 (Calca) | Applied Biosystems, CA, USA |
| CRLR | Mm00516986_m1 (Calcrl) | Applied Biosystems, CA, USA |
| Amelx | Mm00711642_m1 (Amelx) | Applied Biosystems, CA, USA |
| DSPP | Mm00515666_m1 (DSPP) | Applied Biosystems, CA, USA |
| OPN | Mm00436767_m1 (Spp1) | Applied Biosystems, CA, USA |
| OCN | Mm0341825_mH (Bglap) | Applied Biosystems, CA, USA |

*In situ* hybridization DNA fragments list

| Fragment name | GeneBank accession number |
|---|---|
| CGRP | NM_001033954.3 |

Immnohistochmistry antibodies list

| Antigen name | Proprietary name | Source |
|---|---|---|
| CGRP | ENZO BML-CA1134 | Cosmo Bio. Tokyo, Japan |
| Normal rabbit Ig | Dako X0936 | Agilent Tech. CA, USA |

#### 2.2.2. Quantitative real-time RT-PCR

Quantitative real-time RT-PCR was performed using an Applied Biosystems 7300 Fast Real-Time PCR System (Applied Biosystems, CA, USA) according to the manufacturer's instructions. Each amplification mixture (50 μl) contained 100 ng of cDNA, 900 nM forward primer, 900 nM reverse primer, 250 nM fluorogenic probe, and 25 μl of Universal PCR Master Mix (Applied Biosystems, CA, USA). The PCR cycling parameters were 50 °C for 2 min and 95 °C for 10 min, followed by 50 cycles of 95 °C for 15 s and 60 °C for 1 min. The following sequences were amplified: CGRPα, CRLR, AMELX, DSPP, OPN and OCN (Table 1). TaqMan Rodent GAPDH Control Reagents with the VIC Probe were also used (Applied Biosystems, CA, USA). The amplified mouse cDNA levels were normalized to those of GAPDH (rodent GAPDH primers and probes were obtained from "Assays-On-Demand", Applied Biosystems, CA, USA). The threshold cycle (Ct), defined as the cycle at which amplification of the PCR product enters the exponential phase, was determined for each gene by plotting the fluorescence levels *versus* the cycle numbers on a logarithmic scale. The relative expression levels of the genes of interest, namely, CGRPα, CRLR, AMELX, DSPP, OPN and OCN, were estimated by calculating the ΔCt value, defined as the difference in the Ct values of the target genes and the reference gene (GAPDH), according to the manufacturer's recommendations. The ΔCt was inversely proportional to the level of each mRNA transcript present in the muscle samples from the mice. A higher Ct value corresponded to a lower mRNA level. The levels of the amplified mouse cDNAs were expressed as the quantity divided by the Ct value of the same gene at E14.5 on the Y-axis of each graph.

### 2.3. In situ *hybridization*

DNA fragments of CGRP (Table 1) were subcloned into a pGEMT-Easy vector (Promega, USA) and used for the generation of sense or antisense RNA probes. Paraffin-embedded intestinal sections (6 μm) from E14.5, E17.5 and P1 mice were obtained from Genostaff Co., Ltd., Tokyo, Japan. The E14.5, E17.5 and P1 mice were dissected, fixed with Tissue Fixative (Genostaff Co., Ltd., Tokyo, Japan), embedded in paraffin using the manufacturer's proprietary procedures, and cut into 6-μm sections. The tissue sections were then deparaffinized with xylene and rehydrated through an ethanol series and PBS. The sections were fixed with 10% NBF (10% formalin in PBS) for 15 min at RT and then washed with PBS. The sections were treated with 4 μg/ml proteinase K in PBS for 10 min at 37 °C, washed with PBS, refixed with 10% NBF for 15 min at RT, washed with PBS, and placed in 0.2 N HCl for 10 min at RT. After washing with PBS, the

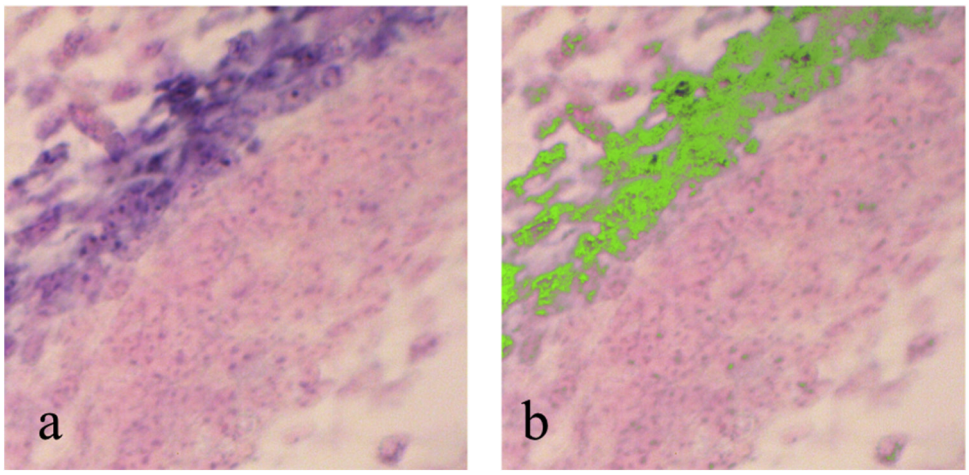


**Fig. 1.** Analysis of images of positive reactions for CGRP mRNA by *in situ* hybridization using an RNA probe coding for CGRP mRNA of tooth in the mouse mandible. All digital images from each slide scanned using a pixel density analysis method modified by Krajewska et al. (2009). The algorithm provides a green-color mark-up image for visualization of a positive reaction. (a) Positive reaction with the CGRP antisense probe image. (b) A green-color mark-up image of Fig. 1a.

sections were placed in 1X G-WASH (Genostaff Co., Ltd., Tokyo, Japan), equivalent to 1X SSC. Hybridization was performed with probes at concentrations of 300 ng/ml in G-Hybo (Genostaff Co., Ltd., Tokyo, Japan) for 16 h at 60 °C. After hybridization, the sections were washed with 1X G-WASH for 10 min at 60 °C, followed by 50% formamide in 1X G-WASH for 10 min at 60 °C. Next, the sections were washed twice with 1X G-WASH for 10 min at 60 °C, twice with 0.1X G-WASH for 10 min at 60 °C, and twice with TBST (0.1% Tween-20 in TBS) at RT. After treatment with 1X G-Block (Genostaff Co., Ltd., Tokyo, Japan) for 15 min at RT, the sections were incubated with anti-DIG-AP conjugate (Roche Diagnostics, USA), diluted 1:2000 with 50X G-Block (Genostaff Co., Ltd., Tokyo, Japan) in TBST for 1 h at RT. The sections were washed twice with TBST and then incubated in a solution containing 100 mM NaCl, 50 mM $MgCl_2$, 0.1% Tween-20, and 100 mM Tris-HCl, pH 9.5. The colorimetric reactions were performed with NBT/BCIP solution (Sigma-Aldrich Co. LLC., USA) overnight and then washed with PBS. The sections were counterstained with Kernechtrot stain solution (Muto Pure Chemicals Co., Ltd., Tokyo, Japan) and mounted with G-Mount (Genostaff Co., Ltd., Tokyo, Japan). Other serial sections at each stage were stained with hematoxylin and eosin. These stained sections were evaluated using microscopy (DM-2500; Leica Microsystems, Bensheim, Germany). We acquired all digital images from each slide by scanning at an absolute magnification of 400 × [resolution of 0.25 μm/pixel (100,000 pix/in.)] in the positive control mandible with tooth germ using a pixel density analysis method (Krajewska et al., 2009). The background illumination levels were also calibrated using a prescan procedure. Each stain by antisense probe that detected CGRPα mRNA was individually calibrated by analyzing single-stained sections and recording optical density (OD) vectors such as staining color. A localization algorithm uses the deconvolution method to separate the stains and classify each pixel according to the number of stains present. The algorithm also provides a green mark-up image for visualization of a positive reaction (Fig. 1) using WinROOF 6.3 (MITANI Corp. Tokyo Japan).

### 2.4. Immunohistochemical staining for anti-CGRPα

CGRP paraffin-embedded blocks for immunohistochemistry were obtained from E14.5 and E17.5 mice from Genostaff Co., Ltd. Mouse embryos were fixed with Tissue Fixative (Genostaff Co., Ltd.), embedded in paraffin using Genostaff's proprietary procedures and cut into 6-μm sections. The tissue sections used for staining with antibody against CGRP were deparaffinized with xylene and rehydrated through a series of ethanol solutions in PBS. Endogenous peroxidases were blocked with 0.3% $H_2O_2$ in methanol for 30 min, followed by incubation with G-Block (Genostaff Co., Ltd.) and the use of an avidin/biotin blocking kit (Vector SP-2001, Vector Laboratories, CA, USA). The sections were then incubated at 4 °C overnight with rabbit polyclonal antibodies against CGRPα (1 μg/ml; ENZO BML-CA1134, Cosmo Bio, Tokyo, Japan) or normal rabbit Ig (Dako X0936, Agilent Technologies, Santa Clara, CA, USA) as a negative control. The sections were washed two times with TBST for 10 min, followed by TBS for 10 min and subsequently incubated with biotin-conjugated goat anti-rabbit Ig (1:600; Dako E0432, Agilent Technologies) at room temperature for 30 min. After washing with TBST and TBS, the sections were incubated with peroxidase-conjugated streptavidin (Nichirei, Tokyo, Japan) at room temperature for 5 min. Peroxidase activity was visualized using diaminobenzidine. The sections were counterstained with Mayer's hematoxylin (MUTO Pure Chemicals Co., Ltd., Tokyo, Japan), dehydrated, and subsequently mounted with Malinol (MUTO Pure Chemicals Co., Ltd.). The stained sections were evaluated using microscopy (DM-2500; Leica Microsystems).

### 2.5. Statistical analysis

Differences in the quantitative real-time RT-PCR data between the experimental groups were assessed using one-way analysis of variance (ANOVA) followed by the Bonferroni post hoc test. The level of significance was set as $p < 0.05$. The results are reported as the means ± SD. All statistical analyses were performed using IBM SPSS Statistics (Base, version 23) (New York, USA).

### 2.6. Ethics

All procedures involving mice were reviewed and approved by the Nippon Medical School Animal Resource Laboratory Committee of the Nippon Dental University (No. 15-31).

## 3. Results

### 3.1. Measurement of mRNA abundance levels using real-time RT-PCR from the mouse mandible containing molar tooth germ

The mRNA abundances of CGRPα, CRLR, AMELX, DSPP, OPN, and OCN in the mandibular body containing molar tooth germ at 5 stages from E14.5 to P1 mice are shown in Fig. 1. The lev-

els of CGRPα mRNA gradually decreased from E14.5 to P1 (E17.5, P0 and P1: p = 0.000; E18.5: p = 0.021) (Fig. 1a). The levels of CRLR mRNA gradually increased from E14.5 to P1 and increased further at E18.5 compared to those at E14.5 (p = 0.000) (Fig. 1b). The AMELX mRNA abundance levels increased from E17.5 onwards (p = 0.000) (Fig. 1c). The DSPP mRNA abundance levels increased more quickly from E17.5 (p = 0.000) to P1 (p = 0.000) than at previous stages, except for those at E18.5 (Fig. 1d). The mRNA abundances of OPN increased from E18.5 to P1 (p = 0.000) (Fig. 1e). The OCN mRNA abundance levels increased rapidly from E18.5 (p = 0.000) to P1 (p = 0.000) (Fig. 1f).

### 3.2. In situ *hybridization in the tooth germ of the mandible*

In the E14.5-stage mice, the tooth bud includes the enamel depression with the thickening of the oral epithelial cells at the surface layer of the mandible (Fig. 3a), and CGRPα mRNA was strongly detected using the antisense probe and found to be located at the epithelial condensed cells between the dental depression and epithelial surface layer of the tooth bud. The antisense probe strongly detected CGRP mRNA both at the enamel depression and between the dental lamina in E14.5 mice (Fig. 4a). The CGRPα mRNA was scattered in the condensed mesenchymal cells beneath the tooth bud at high magnification in Fig. 4a (Fig. 4b). Moreover, CGRP was found to be finely scattered around the alveolar bone matrices at the E14.5 stage using the antisense probe (Fig. 4a, c). At high magnification in Fig. 4a, CGRPα mRNA was strongly detected around the bone matrices and edge of the bone matrices of the mandibular body using the antisense probe (Fig. 4c).

At the E17.5 stage, the tooth germ including the enamel organ with the thickening of the outer and inner enamel epithelium was found in the mandible (Figs. 2 b, 5 a). CGRPα mRNA was strongly detected using the antisense probe in oral epithelial cells near the dental ledge and outer enamel epithelium and scattered at the inner enamel epithelium at the E17.5 stage (Fig. 5b). The membrane shown in Fig. 5c did not show a positive reaction with the antisense probe for CGRPα mRNA between the inner enamel epithelium and dental papilla cells. An intermediate layer with the stellate reticulum showed a weak positive reaction with the antisense probe for CGRPα mRNA between the inner and outer enamel epithelium (Fig. 5d). The finely detected reactions with the antisense probe for CGRPα mRNA were also scattered in the mesenchymal cells of the dental papilla in E17.5 mice (Fig. 5e). A very faint reaction of the antisense probe for CGRPα mRNA was scattered in the condensed mesenchymal cells around bone matrices, mainly located beneath the tooth bud in the mandibular body (Fig. 5f).

At the P1 stage, amnioblast, odontoblast and dental papilla cells were clearly separated in the tooth germ (Figs. 2 c, 6 a). The finely detected reactions with the antisense probe for CGRPα mRNA were found at the apical layer of ameloblasts and odontoblasts and at the dental papilla layers of the P1 stage (Fig. 6b). In the dental papilla layer, a small number of mesenchymal cells that reacted with the antisense probe for CGRPα mRNA were found (Fig. 6c). In contrast, CGRPα mRNA was barely detected around bone matrices and the bone matrices of the mandibular body using the antisense probe at high magnification, as shown in Fig. 6a (Fig. 6d).

Specific signals of the antisense probes for CGRP mRNA were detected in the tooth germ at E14.5 (Fig. 4), E17.5 (Fig. 5) and P1 (Fig. 6) (Table 2).

The antisense probe detected CGRP mRNA of the tooth germ (shown in Table 2) from bud stage to bell stage of the mouse mandible. With the antisense probe, strongly detected CGRP mRNA was obtained in the enamel organ with a bud stage at E12.5. The mRNA level of CGRP was highest in the order dental follicle to dental lamina, dental pulp and dental papilla from E14.5 to P1 mouse tooth germ. Moreover, the mRNA of CGRP was highest in the order ameloblast to odontoblast and dental pulp in the mouse tooth germ organ.

### 3.3. *Immunohistochemistry for CGRP in the mandible*

In the E14.5 mouse, the anti-CGRPα antibody revealed a strong positive reaction at the surface layer of the thickening of the oral epithelial cells in the mandible (Fig. 4d, e). The reaction of the anti-CGRPα antibody was weak at the bone matrices in contrast to the strong mRNA CGRPα expression levels in mesenchymal cells near the bone matrices of the mandibular body at high magnification in Fig. 4a, d (Fig. 4c, f).

In the E17.5 mouse, the anti-CGRPα antibody revealed a strong positive reaction at the thickening of the oral epithelial cells of the dental lamina around the dental ledge depression in the mandibular body (Fig. 5f, g). In the dental follicle, a weak reaction was found in a few mesenchymal cells arranged along the intermediate layer (Fig. 5h). A weak reaction to the anti-CGRPα antibody was also found in a few simple cuboidal epithelia of the outer enamel epithelium (Fig. 5h). Notably, the anti-CGRPα antibody revealed a weak positive reaction in early ameloblasts of the inner enamel epithelium arranged along the intermediate layer between the outer and inner enamel epithelia in E17.5 mice (Fig. 5i, l). In the enamel pulp of E17.5 mice, a very weak reaction to the anti-CGRPα antibody was also found in a few mesenchymal cells near the inner enamel epithelium (Fig. 5i). In the dental papilla, a very weak reaction was also found in a few epithelial cells (Fig. 5l). The weak reaction of anti-CGRPα antibody was detected in the mesenchymal cells around bone matrices of the mandibular body (Fig. 5l). In the immature dentine layer in P1 mice, a weak reaction to the anti-CGRPα antibody was found at the dentine matrices beneath the ameloblasts (Fig. 6g). The reaction to the anti-CGRPα antibody was found in osteoblast-like cells and the mesenchymal cells around bone matrices of the mandibular body (Fig. 6i) in contrast to that of the dental papilla, with no reaction to the anti-CGRPα antibody at P1 (Fig. 6h).

## 4. Discussion

In general, the CGRPα peptide may have direct effects on bone-derived and other surrounding cells (Hukkanen et al., 1993), and CGRP resists bone resorption (Valentijn et al., 1997) and has direct and indirect regulatory effects on the *in vitro* differentiation of osteoblasts (Bo et al., 2012). Fang et al. (2013) indicated that adipose-derived stem cells transduced with adenoviral vectors containing the CGRP gene have a stronger potential to differentiate into osteoblasts *in vitro*. Therefore, CGRPα could be an important marker of osteogenesis and bone resorption. Our data indicated that the antisense probe for CGRPα mRNA showed that CGRPα mRNA was strongly detected at the epithelial condensed cells between the enamel depression and epithelial surface layer of the tooth bud at E14.5 and then scattered in the mesenchymal cells around the enamel and the alveolar bone-like structural zone in E17.5 mice. Finally, CGRPα mRNA was detected in the ameloblast layer and odontoblast layer P1 in the tooth germ. CGRPα mRNA expression was observed during tooth formation at the interfaces between the ectodermal cells of the mandibular epithelium and the underlying neural crest-derived mesenchymal cells during development. In the bone formation stage with developed tooth germ in the mandible, CGRPα mRNA was detected between the dental follicle and outer enamel epithelium at E17.5 in contrast to that of CGRPα mRNA, which was strongly located at the epithelial condensed cells between the dental depression and epithelial surface layer of the tooth bud at E14.5. At the P1 stage, the interfaces between the ectodermal epithelial cells were composed of the

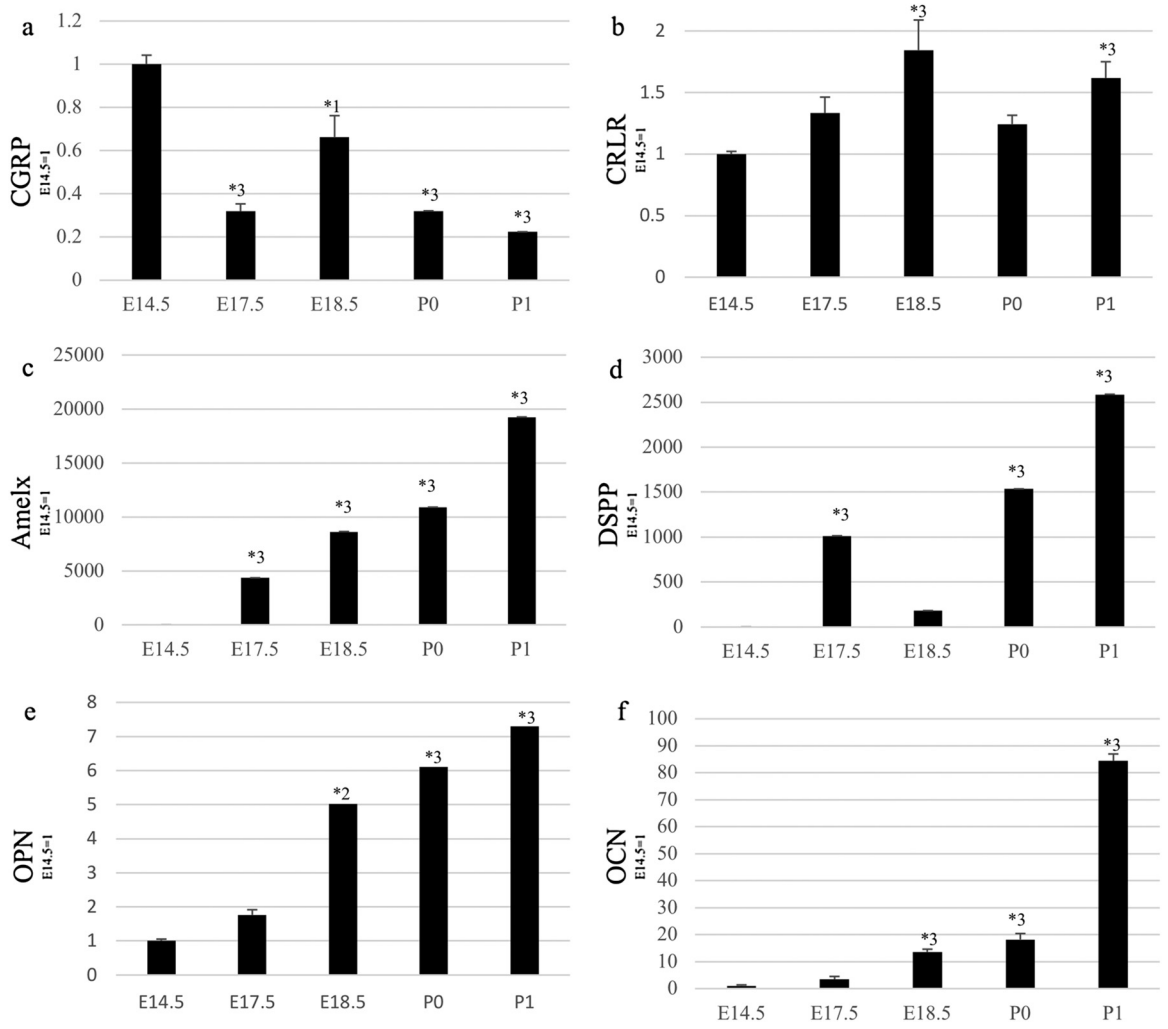


**Fig. 2.** Expression of CGRPα, CRLR, AMELX, DSPP, OPN and OCN mRNAs over time (E14.5, E17.5, E18.5, P0 and P1). The abundances of CGRPα, CRLR, AMELX, DSPP, OPN and OCN mRNAs were normalized to GAPDH at E14.5, E17.5, E18.5, P0 and P1 and subsequently normalized to the target gene expression levels at E14.5. (a) CGRP mRNA expression, (b) CRLR mRNA expression, (c) AMELX mRNA expression, (d) DSPP mRNA expression, (e) OPN mRNA expression, and (f) OCN mRNA expression. Differences between E14.5, E17.5, E18.5, P0 and P1: *1; $p < 0.05$, *2; $p < 0.01$, *3; $p < 0.001$: E14.5 compared to E17.5, E18.5, P0 and P1 stages. All bars represent the mean ± SD.

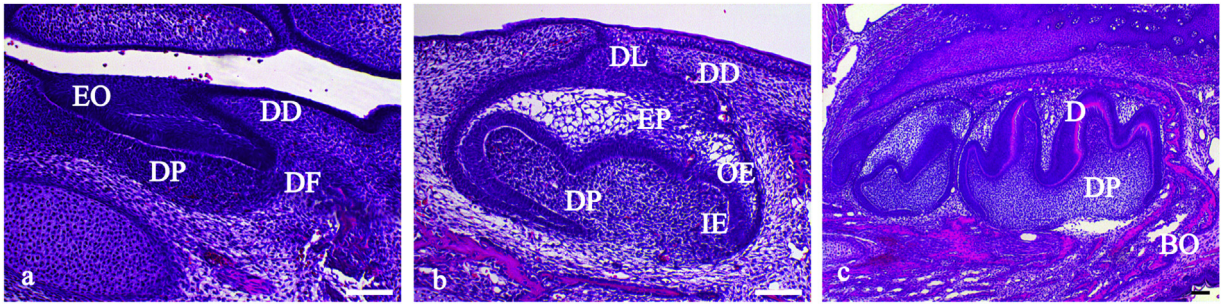


**Fig. 3.** Hematoxylin and eosin (HE) staining of sagittal sections of mouse heads at E14.5 (a) E17.5 (b) and P1 (c) Bo, alveolar bone; D, dentin; DD, dental ledge depression; DF, dental follicle; DL, dental ledge; DP, dental papilla; EO, enamel organ; EP, enamel pulp; IE, inner enamel epithelium; OE, outer enamel epithelium. In a–c, bars = 100 μm.

ameloblast and odontoblast layers from mesenchymal cells in the tooth germ. In each stage, CGRPα mRNA was also detected in the interfaces between ectodermal epithelium and mesenchymal cells of the tooth germ. In the immunohistochemical analyses, CGRPα was found at the surface layer of the oral epithelial cells at E14.5, between dental lamina and mesenchymal cells or inner enamel epithelium at E17.5, and finally at dentine at P1; these specific expression patterns may be associated with neuronal cells that lead to the dentinal tube in tooth germ during development. Therefore, CGRPα may be related to nerve fibers and neuronal cells during formation of the dentinal tube. Of special interest, RT-PCR analysis of mRNA CGRPα expression from E17.5 to E18.5 revealed different levels compared to other stages, with a gradual decrease during development. This is also a specific formation stage with the odontoblast layer *vs.* dental papilla and ameloblast layer *vs.* inner enamel epithelium. CGRPα may also be related to tooth germ development. In general, the nerve branches were directed from the main nerve divisions towards the oral mucosa. Our results show that

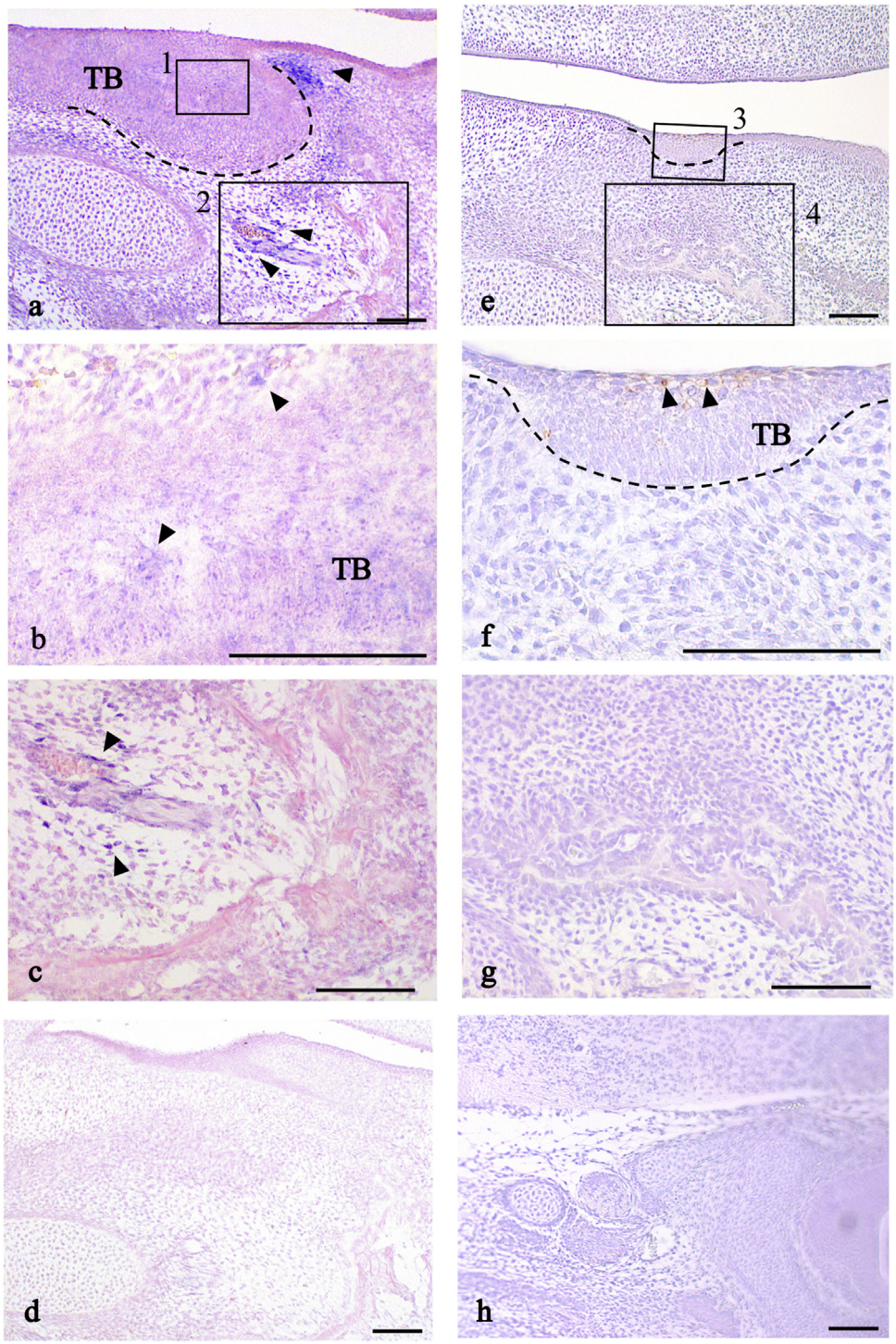


**Fig. 4.** Expression of CGRP mRNA based on the *in situ* hybridization assay with an antisense probe (a, b and c) and a sense probe (d), and immunohistochemical staining for anti-CGRP (e, f and g) and negative control (h) in sagittal sections of E14.5 mice. b (Box 1, see a), c (Box 2, see a), f (Box 3, see e), g (Box 4, see e). E14.5 mice, *in situ* and immunohistochemical staining shows a strong positive reaction (arrowheads) at the surface layer of the thickening of the oral epithelial cells in the mandible. Bo, alveolar bone; DD, dental ledge depression; TB, tooth bud. In a–h, bars = 100 μm.

the antisense probe strongly detected CGRP mRNA mainly in the enamel depression and between the dental lamina at E17.5. Therefore, CGRP, which is a neural marker, may have different roles in the developmental pathway of peripheral nerves that invade the tooth germ. Moreover, the tooth organogenesis markers (DSPP and AMELX mRNAs) were detected in the mouse mandible during development from E14.5 to P1. Therefore, the results from this study suggest that tooth formation occurs in conjunction with the thickening of the oral epithelium of the tooth germ. During development, the nerves were present below the presumptive posterior first molar region, which is in contact with either the oral epithelium or the dental lamina (Mohamed and Atkinson, 1983). Thus, CGRP, along with peripheral nerves, may affect the formation of the dental lamina and dental epithelium in tooth development.

The osteopenia observed in the CGRPα(−/−) mice that have normal levels of calcitonin further show that CGRP is a physiologic

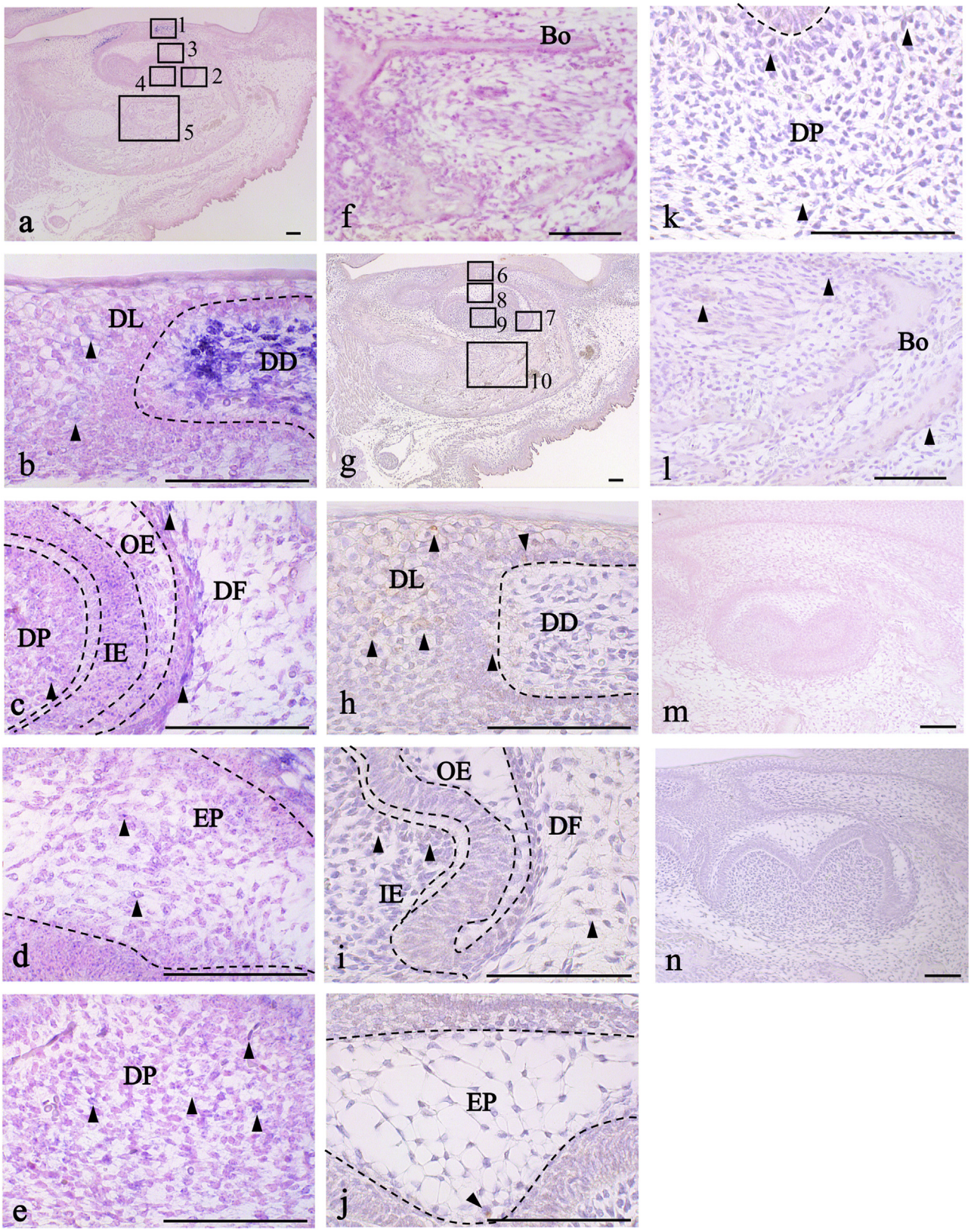


**Fig. 5.** Expression of CGRP mRNA based on the *in situ* hybridization assay with an antisense probe (a–f) and a sense probe (m) and immunohistochemical staining for anti-CGRP (g–l) and negative control (n) in sagittal sections of E17.5 mice. b (Box 1, see a), c (Box 2, see a), d (Box 3, see a), e (Box 4, see a), f (Box 5, see a), h (Box 6, see g), i (Box 7, see g), j (Box 8, see g.), k (Box 9, see g.), l (Box 1 Box 10, see g.) E17.5 mice, *in situ* shows a strong positive reaction (arrowheads) at the thickening of the oral epithelial cells in the dental lamina around the dental ledge depression in the mandible, and immunohistochemical staining shows a weak positive reaction (arrowheads) in early ameloblasts of the inner enamel layer, arranged along the intermediate layer between the outer and inner enamel layers. DD, dental ledge depression; DF, dental follicle; DL, dental ledge; DP, dental papilla; EP, enamel pulp; IE, inner enamel epithelium e; OE, outer enamel epithelium; Bo, alveolar bone. In a–n, bars = 100 μm.

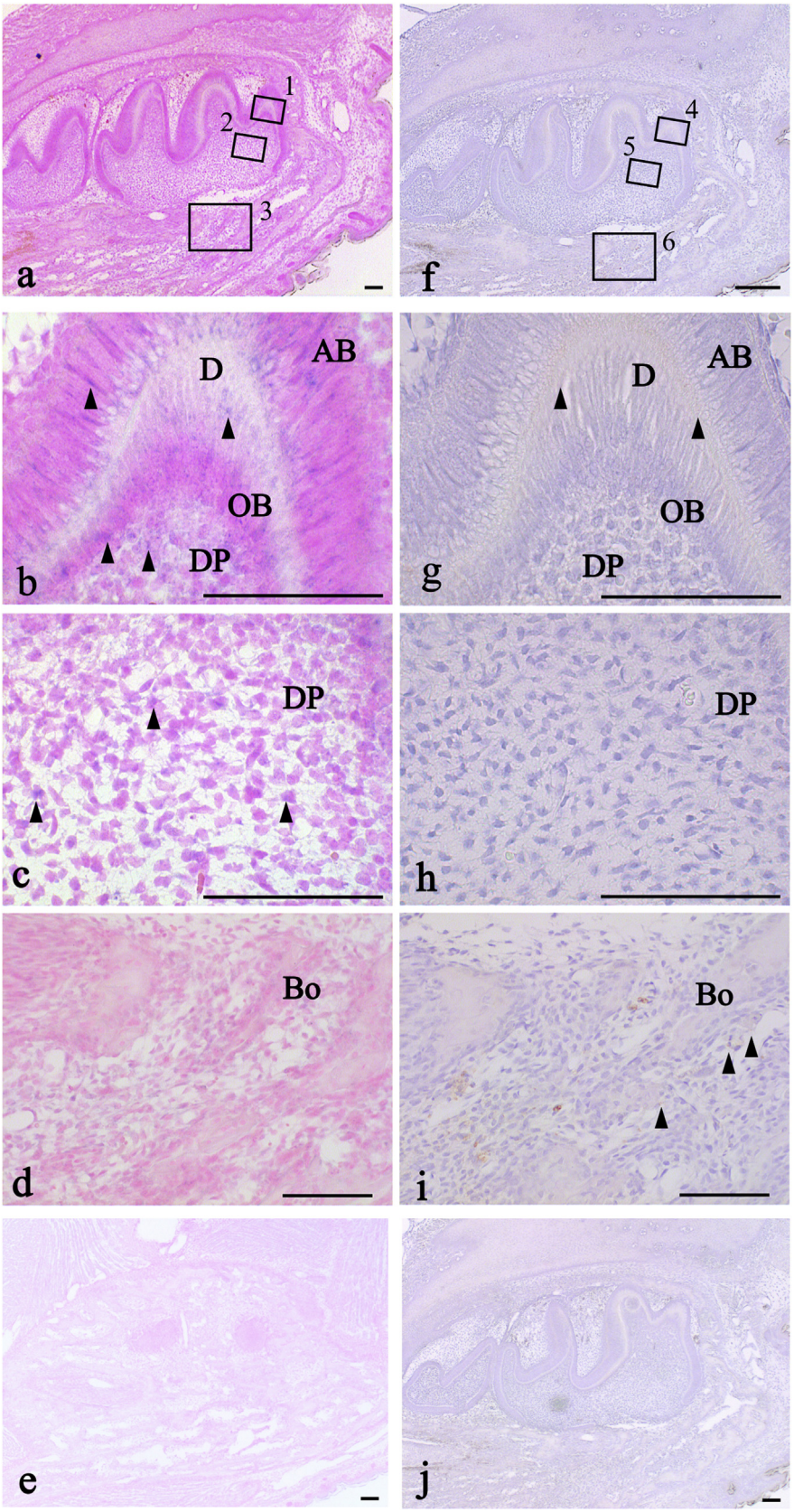


**Fig. 6.** Expression of CGRP mRNA based on the *in situ* hybridization assay with an antisense probe (a–d) and a sense probe (e) and immunohistochemical staining for anti-CGRP (f–i) and negative control (j) in sagittal sections of P1 mice. b (Box 1, see a), c (Box 2, see a), d (Box 3, see a), d2 (box, see d), g (Box 4, see f), h (Box 5, see f), i (Box 6, see f). P1 mice, *in situ* shows a very weak reaction at the dentine matrices beneath the ameloblasts, and immunohistochemical staining shows a weak reaction (arrowheads) in the immature dentine layer and at the dentine matrices beneath the ameloblasts and osteoblast-like cells in the alveolar bone of the mandible. AB, ameloblast; Bo, alveolar bone; D, dentin; DP, dental papilla; OB, osteoblast. In a–j, bars = 100 μm; d2, bar = 100 μm.

**Table 2**
Area percentage of CGRPα reaction list for *in situ*.

| | E14.5 (Bud Stage) | E17.5 (Cap Stage) | P1 (Bell Stage) |
|---|---|---|---|
| Tooth bud | 5.86% ± 1.20 | - | - |
| Dental Follicle | - | 9.14% ± 4.92 | - |
| Dental Lamina | - | 7.77% ± 3.42 | - |
| Stellate reciculum | - | 0.04% ± 0.02 | - |
| Dental Papilla | - | 0.20% ± 0.12 | - |
| Ameloblast | - | - | 18.30% ± 7.69 |
| Odontoblast | - | - | 11.03% ± 5.43 |
| Dental Pulp | - | - | 7.03% ± 4.08 |

It is a proportion of 2,500 $\mu m^2$. *1, $p > 0.05$; *2, $p > 0.005$; *3, $p > 0.001$.

activator of bone formation (Schinke et al., 2004). In general, the bone mass was affected to contain calcitonin and CGRP. CGRP was mainly observed in neuronal cells near the trabecular bone structure in differentiated osteoblast cultures (Schinke et al., 2004). In our results, CGRPα mRNA indicated immature bone matrices in the mandibular body *in vivo*. During mandibular formation, CGRPα is needed for formation of the mandible with bone structures, which is also located at blood vessels. Bone formation in the mandible during growth proceeded from intramembranous bone trabeculae and then changed from woven bone to lamellar bone; in humans, blood vessels also developed at the same time (Sperber, 2001). CGRPα-immunoreactive fibers in bone tissue are associated with blood vessels (Hill and Elde, 1991). CGRPα controls local blood flow, and CGRP-immunoreactive fibers are associated with bone marrow cells, bone cells, and other cells in bone tissue (Hill and Elde, 1991; Irie et al., 2002). That is, vascular and bone development also occurs in conjunction with bone development *in vivo* under the control of CGRPα. The bone matrices were clearly visible from E17.5. CGRPα was located around bone matrices at E17.5 compared to that at E14.5 and P1 in our immunohistochemical data. The antisense probe for CGRP mRNA showed that the reactions were mainly located in the basal region of the tooth germ in the alveolar bone-like structural zone in E17.5 mice. The reactions at the tip of the tooth germ around the mesenchymal cells and the alveolar bone indicated the preparation of tooth eruption during development. The absorption of the bone surrounding the tooth germ might be involved in the regulation of the eruption of tooth germ towards the epithelium. RT-PCR results showed that the OCN mRNA abundance levels increased rapidly from E17.5. Therefore, the period between the E14.5 and E17.5 stages of the mandible may include bone formation of the surrounding tooth germ, which may then temporarily participate as an inhibitor of OCN in bone resorption of the upper region of the tooth germ surrounding the bone from E17.5 of the mouse mandibular body. In contrast, CGRPα mRNA rapidly decreased from E14.5 in contrast to that of OPN, and OCN mRNA was increased from embryonic stage to postnatal stage in the mouse mandible. These results indicated that CGRPα may be negatively related to the osteogenesis markers. Immunohistochemistry and *in situ* hybridization showed the expression of OCN and bone sialoprotein early in the formation of mandibular bone, and they could play a role concomitant with bone matrix mineralization at stages E14-18 (Kamiya et al., 2001). Therefore, OCN is an important mandibular bone matrix formation marker during development. Our results indicated that OCN is also an important marker because it increases in conjunction with the increase in OCN mRNA.

Our results show that CGRP regulates the different roles in the developmental pathway of peripheral nerves that lead to the tooth germ and that occur in conjunction with bone formation.

## Appendix A. Supplementary data

Supplementary data associated with this article can be found, in the online version, at https://doi.org/10.1016/j.aanat.2018.09.001.

## References


Bradaschia-Correa, V., Moreira, M.M., Arana-Chavez, V.E., 2013. Reduced RANKL expression impedes osteoclast activation and tooth eruption in alendronate-treated rats. Cell Tissue Res. 353, 79–86.

Benemei, S., Nicoletti, P., Capone, J.G., De Cesaris, F., Geppetti, P., 2009. Migraine. Handb. Exp. Pharmacol. 194, 75–89.

Bidegain, M., Roos, B.A., Hill, E.L., Howard, G.A., Balkan, W., 1995. Calcitonin gene-related peptide (CGRP) in the developing mouse limb. Endocr. Res. 21, 743–755.

Bjurholm, A., 1991. Neuroendocrine peptides in bone. Int. Orthop. 15, 325–329.

Bo, Y., Yan, L., Gang, Z., Tao, L., Yinghui, T., 2012. Effect of calcitonin gane-related peptide on osteoblast differentiation in an osteoblast and endothelial cell co-culture system. Cell Biol. Int. 36, 909–915.

Cornish, J., Callon, K.E., Lin, C.Q., Xiao, C.L., Gamble, G.D., Cooper, G.J., et al., 1999. Comparison of the effects of calcitonin gene-related peptide and amylin on osteoblasts. J. Bone Miner. Res. 14, 1302–1309.

Dong, J., He, Y., Zhang, X., Wang, L., Sun, T., Zhang, M., et al., 2010. Calcitonin gene-related peptide regulates the glowth of epidermal stem cell in vitro. Peptides 31, 1860–1865.

Edvinsson, L., Ho, T.W., 2010. CGRP receptor antagonism and migraine. Neurotherapeutics 7, 164–175.

Fang, Z., Yang, Q., Xiong, W., Li, G.H., Liao, H., Xiao, J., et al., 2013. Effect of CGRP-adenoviral vector transduction on the osteoblastic differentiation of rat adipose-derived stem cells. PLoS One 8, e72738.

Fontaine, B., Klarsfeld, A., Changeux, J.P., 1986. Calcitonin gene-related peptide, a peptide present in spinal cord motor neurons, increases the number of actylcholine receptors in primary cultures of chick embryo myotubes. Neurosci. Lett. 71, 59–65.

Fristad, I., Heyeraas, K.J., Kvinnsland, I., 1994. Nerve fibres and cells immunoreactive to neurochemical markers in developing rat molars and supporting tissues. Arch. Oral Biol. 39, 633–646.

Haeuchi, Y., Matsumoto, K., Ichikawa, H., Maeda, S., 1999. Immunohistochemical demonstration of neuropeptides in the articular disk of the human temporomandibular joint. Cells Tissues Organs 164, 205–211.

Hill, E.L., Elde, R., 1991. Distribution of CGRP-, VIP-, D beta H-, SP-, and NPY-immunoreactive nerves in the periosteum of the rat. Cell Tissue Res. 264, 469–480.

Hukkanen, M., Konttinen, Y.T., Santavirta, S., Paavolainen, P., Gu, X.H., Terenghi, G., et al., 1993. Rapid proliferation of calcitonin gene-related peptide-immunoreactive nerves during healing of rat tibial fracture suggests neural involvement in bone growth and remodelling. Neuroscience 54, 969–979.

Irie, K., Hara-Irie, F., Ozawa, H., Yajima, T., 2002. Calcitonin gene-related peptide (CGRP)-containing nerve fibers in bone tissue and their involvement in bone remodeling. Microsc. Res. Tech. 58, 85–90.

Kamiya, N., Shigemasa, K., Takagi, M., 2001. Gene expression and immunohistochemical localization of decorin and biglycan in association with early bone formation in the developing mandible. J. Oral Sci. 43, 179–188.

Konttinen, Y., Imai, S., Suda, A., 1996. Neuropeptides and the puzzle of bone. Acta Orthop. Scand. 67, 632–639.

Krajewska, M., Smith, L.H., Rong, J., Huang, X., Hyer, M.L., Zeps, N., Iacopetta, B., Linke, S.P., Olson, A.H., Reed, J.C., Krajewski, S., 2009. Image analysis algorithms for immunohistochemical assessment of cell death events and fibrosis in tissue sections. J. Histochem. Cytochem. 57, 649–663.

Maeda, Y., Miwa, Y., Sato, I., 2017. Expression of CGRP, vasculogenesis and osteogenesis associated mRNAs in the developing mouse mandible and tibia. Eur. J. Histochem. 61, 2750.

Miles, K., Greengard, P., Huganir, R.L., 1989. Calcitonin gene-related peptide regulates phosphorylation of the nicotinic acetylcholine receptor in rat myotubes. Neuron 2, 1517–1524.
Mohamed, S.S., Atkinson, M.E., 1983. A histological study of the innervation of developing mouse teeth. J. Anat. 136, 735–749.
Mulle, C., Benoit, P., Pinset, C., Roa, M., Changeux, J.P., 1988. Calcitonin gene-related peptide enhances the rate of desensitization of the nicotinic acetylcholine receptor in cultured mouse muscle cells. Proc. Natl. Acad. Sci. U. S. A. 85, 5728–5732.
Multon, S., Pardutz, A., Mosen, J., Hua, M.T., Defays, C., Honda, S., et al., 2005. Lack of estrogen increases pain in the trigeminal formalin model: a behavioural and immunocytochemical study of transgenic ArKO mice. Pain 114, 257–265.
Nagata, E., Kondo, T., Ayasaka, N., Nakata, M., Tanaka, T., 1992. Immunohistochemical study of nerve fibres with substance P- or calcitonin gene-related peptide-like immunoreactivity in the junctional epithelium of developing rats. Arch. Oral Biol. 37, 655–662.
Nagata, E., Kondo, T., Kiyoshima, T., Nakata, M., Tanaka, T., 1994. Immunohistochemical evidence for the presence of nerve fibres with substance P- or calcitonin gene-related peptide-like immunoreactivity in the proliferating epithelium in the developing teeth of rats. Arch. Oral Biol. 39, 197–203.
New, H.V., Mudge, A.W., 1986. Calcitonin gene-related peptide regulates muscle acetylcholine receptor synthesis. Nature 323, 809–811.
Russell, F.A., King, R., Smillie, S.J., Kodji, X., Brain, S.D., 2011. Calcitonin gene-related peptide: physiology and pathophysiology. Physiol. Rev. 94, 1099–1142.
Sato, I., Imura, K., Miwa, Y., Yoshida, S., Sunohara, M., 2012. Distributions of calcitonin gene-related peptide and substance P in the human maxillary sinus of Japanese cadavers. J. Craniomaxillofac. Surg. 40, e249–e252.
Schinke, T., Liese, S., Priemel, M., Haberland, M., Schilling, A.F., Catala-Lehnen, P., Blicharski, D., Rueger, J.M., Gagel, R.F., Emeson, R.B., Amling, M., 2004. Decreased bone formation and osteopenia in mice lacking alpha-calcitonin gene-related peptide. J. Bone Miner. Res. 19, 2049–2056.
Sisask, G., Silfverswärd, C.J., Bjurholm, A., Nilsson, O., 2013. Ontogeny of sensory and autonomic nerves in the developing mouse skeleton. Auton Neurosci. 177, 237–243.
Sperber, G.H., 2001. Craniofacial Development. BC Decker Inc., London, p. 128.
Tabarowski, Z., Gibson-Berry, K., Felten, S.Y., 1996. Noradrenergic and peptidergic innervation of the mouse femur bone marrow. Acta Histochem. 98, 453–457.
Takahashi, N., Matsuda, Y., Sato, K., de Jong, P.R., Bertin, S., Tabeta, K., et al., 2016. Neuronal TRPV1 activation regulates alveolar bone resorption by suppressing osteoclastogenesis via CGRP. Sci. Rep. 6, 29294.
Valentijn, K., Gutow, A.P., Troiano, N., Gundberg, C., Gilligan, J.P., Vignery, A., 1997. Effects of calcitonin gene-related peptide on bone turnover in ovariectomized rats. Bone 21, 269–274.
Wise, G.E., 2009. Cellular and molecular basis of tooth eruption. Orthod. Craniofac. Res. 12, 67–73.
Yamazaki, M., Sato, I., 2014. Distribution of substance P and the calcitonin gene-related peptide in the human tensor tympani muscle. Eur. Arch. Otorhinolaryngol. 271, 905–911.
Yoo, Y.M., Kwag, J.H., Kim, K.H., Kim, C.H., 2014. Effects of neuropeptides and mechanical loading on bone cell resorption in vitro. Int. J. Mol. Sci. 15, 5874–5883.